

<https://doi.org/10.51301/ejsu.2026.i1.03>

Dynamics of temperature-strength changes in the immediate roof and formation of the gasified cavity of an underground gasifier

P. Saik^{1,2}, V. Lozynskiy^{1,2*}, M. Berdnyk¹, D. Klimov¹

¹Belt and Road Initiative Center for Chinese-European Studies (BRICCES), Guangdong University of Petrochemical Technology, Maoming, China

²Dnipro University of Technology, Dnipro, Ukraine

*Corresponding author: lozynskiy.v.h@nmu.one

Abstract. This study aims to identify regularities in the evolution of the temperature field and the uniaxial compressive strength (UCS) of immediate roof rocks under the influence of chemical reaction zones along the combustion face. It also aims to determine how the goaf area forms and changes over time as a function of gasification duration, injection pressure of the blowing mixture, and coal seam thickness. The study was carried out using a laboratory UCG setup that reproduces combustion face advance and roof deformation. The temperature in the modelled immediate roof was recorded by sensors installed along the reaction channel. Siltstone samples taken from the immediate roof of seam n_7^n at the Mezhyrichanska mine (SE “Lvivuhillia”, Ukraine) were thermally treated and tested in uniaxial compression using a KL 200/CE-Tecnotest press. The goaf geometry was determined from roof-subsidence reference sensors, graphical reconstruction of contours at different time instants, and area calculation by the trapezoidal rule with consideration of producer-gas composition and concentration. At 0.55 m above the seam, temperature in the oxidizing zone (0-9 m) increased from approximately 323 to 550°C, reached about 573°C in the transition zone (9-11 m), and decreased to ~200°C in the reducing zone (11-30 m). UCS varied along the combustion face with a maximum near the transition zone and a subsequent decrease in the reducing zone. An exponential relationship was observed in the oxidizing zone, whereas a logarithmic relationship was observed in the reducing zone. The goaf area changed nonlinearly, predominantly exponentially, with gasification duration and seam thickness. It was also associated with the injection-pressure regime of the blowing mixture and roof-caving manifestations. The identified relationships can be used to predict goaf parameters and to assess roof stability when substantiating controlled UCG operating regimes.

Keywords: *underground coal gasification; goaf; temperature field; rocks; uniaxial compressive strength; combustion face.*

Received: 14 August 2025

Accepted: 2 February 2026

Available online: 28 February 2026

1. Introduction

Today, underground coal gasification is regarded as one of the promising technologies that enables the rational use of a substantial part of the resource base that was previously considered economically impractical or technically unsafe for conventional mining [1, 2]. One of the key advantages of underground coal gasification is a significant reduction in anthropogenic pressure on mining regions [3, 4]. Unlike conventional mining, underground gasification does not require the development of underground workings, hoisting of rock mass to the surface, or the creation of waste rock dumps, sludge ponds, or tailings storage facilities. As a result, the area of technogenically disturbed land is substantially reduced, the scale of potentially hazardous geoenvironmental objects is limited, and the risk of adverse environmental impacts is reduced [5-9]. Another essential advantage is improved industrial safety. Since the main processes occur without personnel in underground space, the primary hazards typical of conventional underground coal mining are eliminated, including gas-dynamic events, roof falls, sudden outbursts, and methane or coal-dust explosions [10-12].

The implementation of underground coal gasification is particularly relevant for the coal-mining regions of Ukraine, where a considerable share of reserves occurs under challenging mining and geological conditions, including thin seams, significant depths, and previously mined or otherwise hazardous zones [13-15]. Under such conditions, underground gasification may become one of the key directions for transforming the coal sector by combining energy efficiency with environmental and technical safety.

The efficiency, stability, and safety of this process are determined mainly by the parameters of the underground gasifier, where complex coupled thermal, physico-chemical, and gas-dynamic processes develop within the rock mass [16-18]. In this context, studying the geomechanical stability of the rock mass under the action of thermal and chemical processes accompanying gasification becomes especially important. Because the behaviour of the immediate roof rocks governs the stability of the reaction cavity, the safe operation of the gasifier, and the overall process performance, their condition requires comprehensive and rigorous integrated investigations.

© 2026. P Saik, V. Lozynskiy, M. Berdnyk, D. Klimov

saik.p.b@nmu.one; lozynskiy.v.h@nmu.one; berdnyk.m.g@nmu.one; klimov.d.h@nmu.one

Engineering Journal of Satbayev University. eISSN 2959-2348. Published by Satbayev University

This is an Open Access article distributed under the terms of the Creative Commons Attribution License (<http://creativecommons.org/licenses/by/4.0/>), which permits unrestricted reuse, distribution, and reproduction in any medium, provided the original work is properly cited.

In addition to purely technological factors, the relevance of underground coal gasification is strengthened by the need to ensure energy resilience and flexibility of energy supply systems under instability, where the role of decentralised approaches and optimisation of power generation control is increasing [19]. At the same time, the efficiency and controllability of the UCG process depend on the correct consideration of mass and heat balances in the reaction channel. This is particularly important under complicated geological conditions, including discontinuities and faults, which directly affect the formation of temperature fields and the energy performance of gasification [20, 21].

One of the key characteristics of underground gasifier operation is the formation of the gasification goaf, which directly influences the intensity of gasification reactions, the conditions of heat and mass transfer, and the filtration properties of the rock mass [22, 23]. The evolution of the gasification goaf is nonlinear. It is governed by the combined effects of mining and geological conditions, the physico-chemical properties of coal, the composition of blowing mixtures, reactant injection regimes, and the thermodynamic parameters of the process [24].

2. Literature review

The influence of high temperatures on the physico-mechanical properties of rocks is intensively studied in contemporary scientific literature. This interest is driven by the development of high-temperature mining technologies, in particular underground coal gasification and in situ coal combustion [22-24]. The implementation of these technologies is accompanied by substantial thermal, gas-dynamic, and chemical impacts on the coal seam and surrounding rocks. As a result, the stress-strain state changes, and strength parameters within the rock mass are redistributed [25-28]. The relevance of investigating rock-mass strength dynamics stems from the fact that roof and surrounding-rock stability within the thermally affected zone is a critical factor for predicting potential deformations, preventing uncontrolled caving, defining the boundaries of the reaction cavity, and assessing process safety. Under the combined action of high temperatures, thermochemical decomposition, and the formation of secondary porosity, the mechanical properties of rocks may vary over a wide range. This requires a comprehensive analysis that accounts for the rock mass's temporal and spatial heterogeneity. Therefore, given the growing interest in coal thermochemical conversion technologies in Ukraine and worldwide, assessing rock strength characteristics is particularly important.

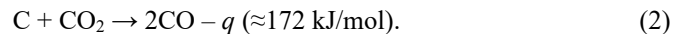
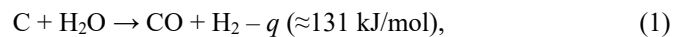
Understanding the regularities of strength degradation in the rock mass and the formation of weakened zones is essential for developing reliable geomechanical models, optimising gasification operating regimes, and preparing recommendations for industrial implementation [29]. Studying the dynamics of rock-mass strength during underground coal gasification is an important scientific and applied task that provides a basis for improving the safety, efficiency, and controllability of these geotechnologies.

In contrast to combustion, underground gasification enables a controlled thermal regime and a more uniform distribution of chemical reaction zones along the reaction channel [30-32]. This can substantially reduce the thermal load on the rock mass and ensure a more stable development process,

thereby improving overall safety. Underground coal gasification is characterised by continuous formation and migration of active zones within the reaction channel. Their dynamics are governed primarily by the temperature field in the underground gasifier. Experimental and laboratory studies [33, 34] describe the spatiotemporal temperature distribution around the gasifier in detail and demonstrate a consistent pattern of evolution that corresponds to the progression of chemical reactions across different sections of the reaction channel. Temperature variations determine the character, intensity, and position of the oxidizing and reducing zones, which, in turn, control thermochemical transformations and the geomechanical state of the surrounding rocks [35].

Laboratory and analytical studies have shown that the temperature gradient along the reaction channel varies widely depending on reaction activity [36-38]. In the oxidizing zone, the temperature ranges from 600 to 1050 °C. This zone is characterised by intensive exothermic oxidation of carbon ($C + O_2 \rightarrow CO_2 + q$, where $q \approx 394$ kJ/mol), which provides the primary input of thermal energy to the system. The temperature gradient within this section is 25-50°C/m, which is explained by the high rate of heat release concentrated in a limited volume.

Endothermic reactions, in particular, characterise the reducing zone:



In this part of the channel, the temperature gradually decreases to 412°C, and the gradient is 15-20°C/m. The lower rate of change is due to reactions consuming heat and to the limited availability of reagents from the blowing mixture. The transition zone between the exothermic and endothermic intervals is significant because it produces the most tremendous thermal impact on the rock mass. This zone is associated with peak thermal loading, resulting in the most intense changes in rock geomechanical properties.

Today, despite a substantial body of research on underground coal gasification, systematic investigation of the gasification goaf dynamics remains underdeveloped. Most existing approaches focus on individual aspects of the process, in particular on generalised characteristics of goaf growth [39]. They do not provide a unified methodological basis for analysing its temporal evolution and its expansion relative to the chemical reaction zones within an underground gasifier [40]. For example, study [41] substantiated the parameters governing the formation of bedding-separation cavities in roof rocks during underground coal gasification and established their dependence on reaction channel length. However, that approach did not account for the spatial arrangement of chemical reaction zones along the reaction channel, thereby limiting the scope for a comprehensive analysis of gasification goaf dynamics. Study [42] identified regularities in the formation of the gasification goaf during coal gasification through vertical wells. At the same time, the reported goaf parameters mainly describe the final stage of the process, namely the attenuation of gasification operations, which restricts analysis of the active stage. The authors of [43] demonstrated that the parameters of the gasification goaf, including its shape, dimensions, and the spatial position of active zones, are closely related to gasification process control regimes. This supports the need to predict gasification goaf geometry based on thermal and technological parameters as a prerequisite for improving controllability UCG.

Most studies on the effect of temperature on the physico-mechanical properties of rocks have been conducted under laboratory conditions [44, 45]. They typically do not account for the spatial variation of the temperature field along the combustion face of an underground gasifier. In many cases, the results of such experiments have been considered separately from the actual conditions that govern the formation of chemical reaction zones. This complicates direct transfer of the obtained data to field-scale objects [46-48]. At the same time, research on the effects of temperature on rock properties shows both common trends and pronounced differences. This allows the identification of regularities in the evolution of strength as a function of rock type, mineralogical composition, and structural features. In particular, most sedimentary rocks exhibit an initial increase in strength due to dehydration and changes in intercrystalline contacts. At higher temperatures, however, structural rearrangement, mineral decomposition, and crack formation are observed [49-52].

Study [53] established a clear relationship between temperature and sandstone strength. As the temperature increased from 25 to 800°C, the uniaxial compressive strength decreased from 95.6 to 49.5 MPa. A similar trend was reported for the elastic modulus, which decreased after 200°C and 400°C. The authors attributed these changes to rock dehydration, microcrack development, and the subsequent thermal decomposition of quartz and feldspar. Research [54] confirmed a reduction in sandstone tensile strength during heating. Up to 500°C, the changes remained relatively stable, whereas at 600°C, a sharp drop in strength of 22-23% was observed. Study [55] examined the behaviour of marble, limestone, and sandstone. The authors noted that the peak strength and elastic modulus of carbonate rocks decrease after 200-400°C, and that a sharp deterioration in mechanical properties occurs after 600°C. It was also emphasised that peak strain increases markedly when rocks are heated above 600°C. In [56] and [57], it was reported that the strength evolution depends strongly on rock mineralogy. Carbonate rocks may temporarily strengthen when heated to 150°C. With further temperature increases, dehydration begins, and intensive microcracking develops. Study [58] found that granite strength decreases by 80% when heated to 1000°C. The most pronounced change occurs in the 400-600°C range, which the authors associated with the quartz phase transition at 573°C.

Results for sandstone heated to 1100°C [59] indicate a more complex response. Strength increases up to 400°C by nearly a factor of two, but then drops sharply to 26 MPa. Claystone specimens show a different pattern. When heated to 400°C, strength increases due to water evaporation and rock densification, but above 400°C, it rapidly decreases, reaching 70 MPa [60]. Study [61] reported data on clay- and sandy-shale samples heated to 1000°C, where strength increased, attributed to dehydration and decarboxylation reactions. Studies on limestone properties [62] indicate that significant strength loss occurs already at 100°C, while further heating to 700-800°C produces little additional change in load-bearing capacity. Study [63] analysed changes in sandstone strength and permeability. Both were reported to increase up to 200°C, after which mechanical properties deteriorated due to microcrack development. Investigations of residual strains in sandstone at 700-1200°C [64] showed a sharp increase caused by profound changes in rock structure.

A synthesis of the above studies indicates that the effect of temperature on rock mechanical properties is complex and nonlinear. It depends strongly on mineralogical composition, texture, porosity, and the specific mechanisms of thermally induced reactions. Temperature-driven changes may manifest as temporary strengthening, especially in water-bearing rocks, or as abrupt structural weakening once critical temperature thresholds are reached. These thresholds are commonly associated with phase transformations and thermal decomposition of minerals [65]. Therefore, specialised experimental investigations are required for each specific mining and geological setting to account for rock-specific behaviour.

At the same time, without linking laboratory-derived regularities to the actual temperature distribution along the reaction channel of an underground gasifier, it is not possible to adequately reproduce the rock mass's mechanical response under UCG conditions. This emphasises the need for integrated studies that consider the spatial arrangement of chemical reaction zones, the nature of temperature gradients, and their influence on roof conditions. Such studies should also address the associated parameters governing gasification goaf formation in underground gasifiers. Because goaf geometry evolves in space and time and results from coupled thermal and geomechanical processes, its dynamics should be treated as an integral component when assessing reaction-cavity stability and gasification controllability. In this regard, an important scientific and practical task is to investigate the dynamics of the gasification goaf in an underground gasifier. Such investigations provide an integrated framework for analysing the temporal evolution of its parameters and lay the groundwork for improving the controllability and predictability of the underground gasification process.

In view of the above, this article aims to investigate changes in the strength characteristics of the immediate roof rocks of an underground gasifier due to high-temperature chemical reaction zones along the combustion face. It also aims to establish regularities in the formation and evolution of the gasification goaf area in space and time as a function of gasification duration and coal seam thickness.

Achieving this aim requires solving the following interrelated tasks:

- to determine the temperature dependence in the immediate roof rocks of the underground gasifier;
- to examine changes in the strength characteristics of the immediate roof of the underground gasifier along the combustion face length, where the roof is represented by siltstone;
- to propose a method for calculating the gasification goaf area of the underground gasifier;
- to establish relationships describing the formation and evolution of the gasification goaf area as a function of gasification duration and coal seam thickness.

3. Materials and methods

3.1. Temperature field and strength testing of the immediate roof rocks

The temperature-field distribution was investigated using a dedicated bench-scale test rig designed to reproduce conditions close to those of underground coal gasification [66]. Temperature was recorded by thermocouples embedded in the modelled immediate roof of the laboratory gasifier, which provided reliable data on the thermal regime along the reaction channel.

Changes in the physico-mechanical properties of the rock mass were evaluated through laboratory testing of rock samples collected from the immediate roof of seam n_7^n at the Mezhyrichanska mine of SE “Lvivuhillia” (Ukraine). The immediate roof is represented by siltstone. This choice was motivated by the fact that, in most mines in the region, the immediate roof rock consists of approximately 80% siltstone, with claystone and sandstone each accounting for about 10%. The collected rock fragments were pre-processed using a TCM350 stone-cutting machine to prepare samples with the required geometry for further testing.

Heating prepared samples batches simulated thermal impact in an electric muffle furnace to preset temperatures characteristic of different chemical reaction zones along the combustion face of the underground gasifier. The investigated temperature range covered values typical of the chemical reaction zones in the underground gasifier. These values were defined at a distance of 0.55 m above the seam, which corresponds to half the thickness of the siltstone layer in the immediate roof.

This approach enabled reproducing the thermal impact on the rock under conditions as close as possible to natural ones. It enabled an objective assessment of how increased temperature affects the physico-mechanical properties of the rock mass within the underground gasifier's influence zone. The general view of the selected rock samples and their condition during laboratory testing is shown in Figure 1.

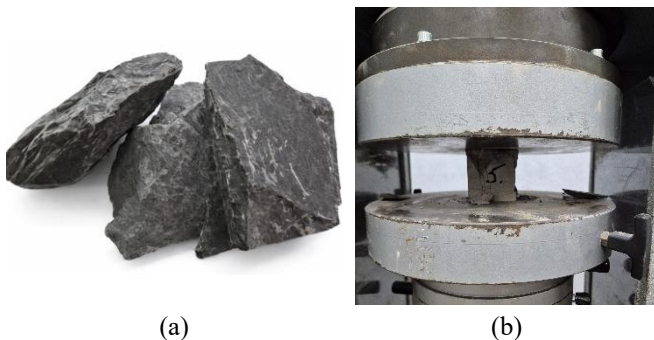


Figure 1. General view of the selected rock samples (a) and the strength testing procedure (b)

Uniaxial compressive strength was determined using a KL 200/CE-Tecnotest testing press, which provides high-precision load control and enables reliable evaluation of rock mechanical behaviour before and after thermal treatment.

3.2. Determination of gasified space parameters during laboratory UCG modeling

The advance rate of the combustion face governs the dimensions of the gasification goaf in an underground gasifier. This rate is a variable parameter and depends on the location and activity of the chemical reaction zones. During the investigation of underground coal gasification, the following were determined. These included combustion face displacement parameters as a function of gasification duration, roof subsidence parameters in the underground gasifier, and the concentrations of combustible gases (CO, H₂, CH₄) in the producer gas.

Roof subsidence parameters were established from displacement measurements of reference sensors installed in the modelled immediate roof of the underground gasifier under laboratory conditions. The use of these sensors enabled accurate tracking of rock deformation and real-time analysis of

accumulated laboratory data. Based on the maximum roof subsidence data over a given time interval, a detailed graphical reconstruction of the gasification goaf was performed. This reconstruction reflected the dynamics of combustion face advance. It enabled the identification of potential roof-caving zones and supported real-time assessment of structural changes in the underground gasifier's roof. Figure 2 presents an example schematic illustrating combustion face advance and the formation of the gasification goaf.

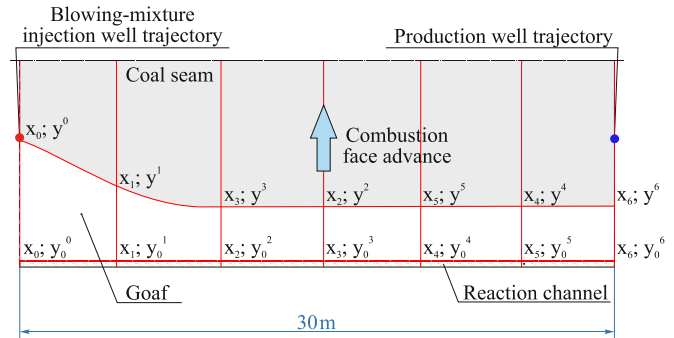


Figure 2. Schematic of combustion face advance and gasification goaf formation

Based on the obtained data (Figure 2) on the combustion face position $(x_0, y^0; \dots x_6, y^6)$ and the reaction channel position $(x_0, y_0^0; \dots; x_6, y_0^6)$, the area of the gasification goaf of the underground gasifier and the area of collapsed rocks are determined. During underground coal gasification, it is reasonable to distinguish three main zones within the gasification goaf. Each zone exhibits both standard and distinct features that govern the process behaviour.

The first zone is the combustion face zone, which is characterised by the combustion face area S_f . It forms adjacent to the combustion face and extends into the gasification goaf. The zone depends on the combustion face advance rate and the roof-caving step. It is the most active zone and the most critical for process control because the main chemical reactions converting coal into producer gas occur there.

The second zone is the caving zone, which is characterised by the caving area S_c . It covers regions where roof rocks lose stability and may collapse, potentially altering the geometry of the underground gasifier.

The third zone is the total gasification goaf area, ΣS , which encompasses the entire region where underground coal gasification occurs.

For optimising the blowing-mixture injection parameters, the S_f value is important. It is determined using the following equation:

$$S_f = \Sigma S - S_c, \text{ m}^2. \quad (3)$$

The boundaries of variation of ΣS are defined by the combustion face position, its length, and the reaction channel position. When these parameters are considered in a coordinate system, x represents the locations of the reference sensors along the combustion face length (30 m with a 5 m spacing). The coordinate y represents the combustion face position within the gasification panel. It changes over time and depends on the chemical reaction zone along the combustion face. The coordinate y_0 denotes the reaction channel position. Based on these coordinates, the gasification goaf area can be determined using the trapezoidal rule. As an example, the procedure for calculating the area of the ΣS zone is given below.

Area between the coordinates (x_0, y^0) and (x_1, y^1) :

$$S_{x_0-x_1} = \frac{(y^0 + y^1)(x_1 - x_0)}{2}, \text{ m}^2; \tag{4}$$

Area between the coordinates (x_1, y^1) and (x_2, y^2) :

$$S_{x_1-x_2} = \frac{(y^1 + y^2)(x_2 - x_1)}{2}, \text{ m}^2; \tag{5}$$

Area between the coordinates (x_5, y^5) and (x_6, y^6) :

$$S_{x_5-x_6} = \frac{(y^5 + y^6)(x_6 - x_5)}{2}, \text{ m}^2; \tag{5}$$

$$\Sigma S = S_{x_0-x_1} + S_{x_1-x_2} + \dots + S_{x_5-x_6}, \text{ m}^2; \tag{6}$$

The parameters of the S_c zone are determined using the same calculation scheme.

The calculated areas ΣS , S_f , and S_c characterise both the development of the gasified space and the onset of caving within the modelled roof. This enables the process to be interpreted in terms of controllability, because changes in S_f reflect the active reaction region that responds to the blowing-mixture regime. The following section presents the results and discusses the relationships among the gasified space evolution, the thermal field, and the roof-rock behaviour.

4. Results and discussion

4.1. Temperature field and strength variation of the immediate roof rocks

As a result of the conducted studies, data were obtained on the variation in the temperature field in the immediate roof rocks along the combustion face, at a distance of 0.55 m above the coal seam (Figure 3).

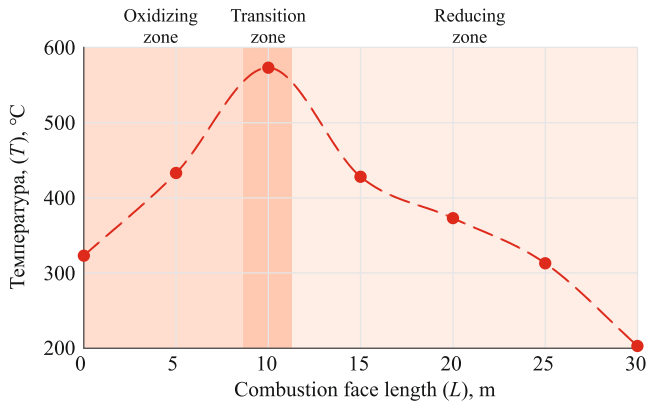


Figure 3. Dynamics of temperature variation in the immediate roof rocks

According to the analysis of the data shown in Figure 3, within the oxidizing zone (0-9 m), the temperature increases from approximately 320 to 550°C. This corresponds to the intensive development of exothermic carbon-oxidation reactions, which release substantial heat. At a distance of 9-11 m, the maximum temperature gradient is recorded. This interval corresponds to the transition zone, where the temperature reaches 575°C. In the reducing zone (11-30 m), the temperature gradually decreases to 200°C. This decline results from endothermic reduction reactions, during which heat is actively absorbed.

The obtained results are consistent with previous studies reporting an asymmetric temperature-field distribution in the rock mass surrounding an underground gasifier. This asymmetry is caused by changes in the type and intensity of chemical reactions along the combustion face, which produces a complex spatial pattern of thermal impact on the roof rocks.

Further analysis that accounted for the spatial temperature distribution enabled the identification of regularities in the variation of rock strength characteristics along the combustion face length. This approach reproduced the actual pattern of thermal impact on the rock mass and enabled evaluation of the degree of weakening in the corresponding chemical reaction zones. This is critical for predicting rock-mass stability during underground gasifier operation. The dependence of the uniaxial compressive strength of rock specimens from the Mezhyrichanska mine of SE “Lvivuhillia” on temperature, which corresponds to different chemical reaction zones of underground coal gasification, is shown in Figure 4.

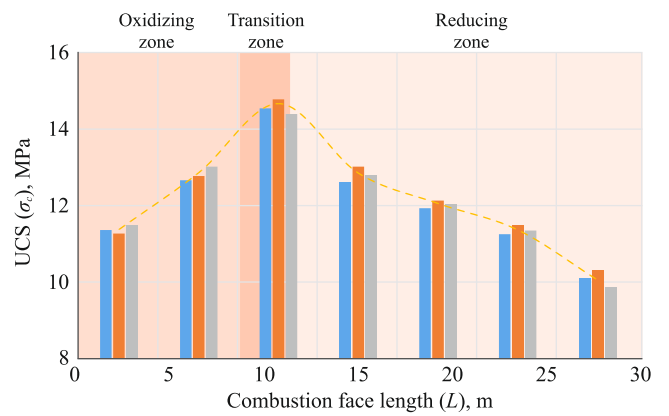


Figure 4. Data on the variation in rock uniaxial compressive strength across the chemical-reaction zones of underground coal gasification: 1-3 – rock samples; 4 – averaged value

Analysis of the data in Figure 4 shows a clear relationship between rock strength variation and temperature along the combustion face. In the oxidizing zone (0-9 m), strength increases. At 0 m, which corresponds to the location of the injection well, the average values are 11.3-11.5 MPa. At 5 m, strength increases to 12.7-13.1 MPa. At 10 m, corresponding to the maximum thermal impact within the transition zone, a strength peak of 14.50-14.89 MPa is observed, with an average strength of 14.8 MPa. In the reducing zone (11-30 m), strength decreases gradually from 12.9 to 10.1 MPa. The minimum values of 9.9-10.4 MPa correspond to the location of the production well of the underground gasifier. Therefore, along the combustion face length, the uniaxial compressive strength varies according to a polynomial relationship as follows:

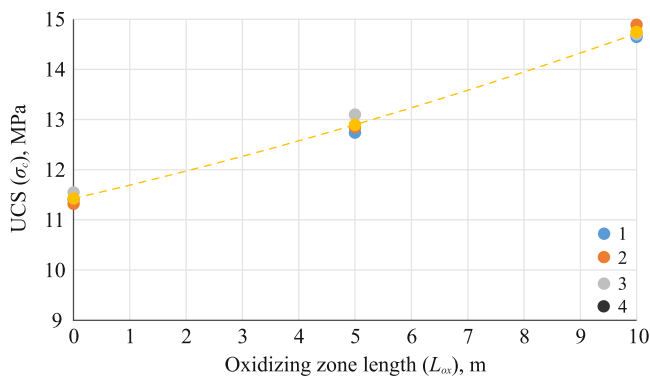
$$UCS_c = 11.8 + 0.28L - 0.01L^2, \text{ MPa}, \tag{7}$$

where L is the combustion face length, m.

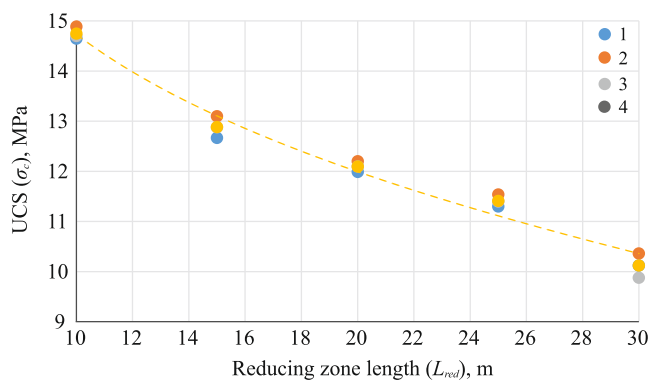
Along the combustion face of the underground gasifier, rock strength varies widely due to differences in the physico-chemical processes in the corresponding reaction zones. Therefore, it is more appropriate to evaluate strength parameters separately for each interval rather than generalise them using a single polynomial relationship. With these considerations, separate relationships were obtained for the strength variation of the immediate roof rocks of the underground

gasifier for different chemical reaction zones. This enabled a more accurate description of rock mechanical behaviour under the temperature conditions characteristic of the oxidizing, transition, and reducing sections of the reaction channel.

Two characteristic temperature ranges were identified. The first range corresponds to the oxidizing zone and is characterized by a gradual increase in rock strength due to dehydration, partial densification, and strengthening of intercrystalline contacts. The second range corresponds to the reducing zone, where the temperature variation along the combustion face length results in only a minor increase in rock strength. Such a separation of temperature intervals enabled the correct interpretation of the results and the development of relationships that reflect the actual strength changes in the immediate roof rocks during underground coal gasification. The obtained results are shown in Figure 5.



(a)



(b)

Figure 5. Variation in the uniaxial compressive strength of rocks along the length of the combustion face as a function of the temperatures in the chemical-reaction zones: (a) – oxidizing zone; (b) – reducing zone: 1-3 – rock samples; 4 – averaged value

Analysis of the data in Figure 5 shows that an exponential relationship of the form describes the strength variation in the oxidizing zone (a):

$$UCS_c^{ox} = 11.4 \exp(0.023L^{ox}), \text{ MPa}, \quad (7)$$

where L_{ox} is the length of the oxidizing zone of the combustion face, m.

This curve shape reflects an intensive increase in strength under temperatures typical of this section of the reaction channel, where dehydration processes and changes in intercrystalline bonds dominate. In contrast, the strength variation of the immediate roof rocks in the reducing zone is described by a logarithmic relationship of the form:

$$UCS_c^{red} = 23.8 - 3.9 \ln(L^{red}), \text{ MPa}, \quad (8)$$

where L_{red} is the length of the reducing zone of the combustion face, m.

Within the oxidizing zone up to the transition zone, the temperature rise leads to a 22-38% increase in rock strength compared with the initial mean value of 9.1 MPa. The maximum strength is reached in the transition zone of the underground gasifier. After that, towards the production well, the values begin to decrease. In the plane of the production well, the average rock strength increased by 10% (1.0 MPa). In general, an increase in the strength of the immediate roof rocks directly improves the overall stability of the rock mass. Stronger rocks can more effectively carry and redistribute stresses that arise during the formation of the reaction cavity in the underground gasifier. As a result, the probability of deformations, subsidence, and local caving is reduced, providing more stable operating conditions for the underground gasifier and improving operational safety.

4.2. Dynamics of gasified space formation and its relation to process control

Based on the obtained data, each experimental series included not only a graphical reconstruction of combustion face advance but also a detailed analysis of the formation of the gasified space over time. This covered the dynamics of temperature, pressure, and gas concentrations at different stages of gasification. In total, 216 graphical representations of process dynamics were developed. They enable determining the gasified area as a function of time, including the stage associated with roof caving, using the trapezoidal rule. Sectional profiles of the gasified space were also analysed, which enabled the accurate determination of its geometric parameters.

The data in Figure 6a indicate that after 6 h of gasification, the gasified space area is 12.6 m². When the reaction channel area is included, the total area equals 18.6 m². The combustion face advance rate is 0.07 m/h. The combustion face is linear, and the oxidizing-zone length is $L_{ox} = 9.0$ m. The blowing-mixture injection pressure is 0.4 MPa. The concentration of combustible gases is 37.9%.

During further gasification of the coal seam, an acceleration of combustion face advance in the oxidizing zone is observed (Figure 6b). At 10.5 h of gasification, a decrease in the concentration of combustible gases to 37.2% was recorded. For this reason, a decision was made to increase the blowing-mixture injection pressure. At an average pressure of 0.45 MPa, the concentration of combustible gases increased to 38.5% at 12.0 h of gasification. This indicates active interaction between the blowing-mixture components and the coal seam surface. An increase in pressure intensifies interphase contact, thereby promoting thermochemical gasification reactions.

Under these conditions, the gasified space area is 32.5 m². For a coal seam thickness of 1.0 m, the pressure increase of the blowing mixture started at 9.0 h of the process. For seam thicknesses of 0.8 m and 0.6 m, it started at 6.8 h and 5.8 h, respectively. The corresponding gasified space areas were 31.2 m², 32.1 m², and 34.2 m².

It should be noted that throughout the gasification process, which lasted 16.4 h (Fig. 6c), the gasified area increased, resulting in a total increase of 7.5 m².

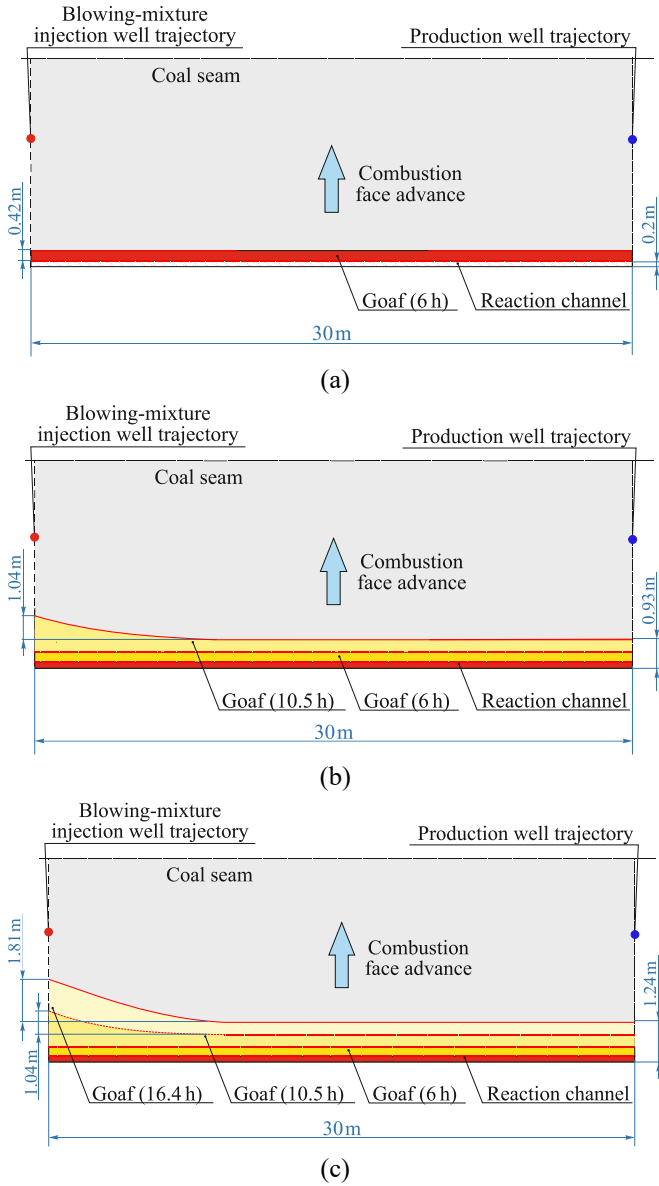


Figure 6. Schematic of combustion face advance at coal seam thickness $m = 1.2$ m, and blowing-mixture injection pressure $P = 0.45$ MPa for different gasification durations (a) – 6.0 h; (b) – 10.5 h; (c) – 16.4 h

This increase occurred while the blowing-mixture injection pressure remained stable at 0.45 MPa, which indicates high gasification efficiency under the given conditions. At 19.8 h of gasification, the concentration of combustible gases began to decrease, reaching 37.5%. Therefore, the blowing-mixture injection pressure was increased to 0.57 MPa. The gasified space area reached 53.0 m². For a seam thickness of 1.0 m, the pressure increase started at 16.9 h. For seam thicknesses of 0.8 m and 0.6 m, it started at 14.2 h and 11.2 h, respectively. The corresponding gasified space areas were 52.5 m², 53.4 m², and 51.5 m². The average blowing-mixture injection pressure was 0.57 MPa.

With further growth of the gasified space to 60.4 m² at 23.7 h (Figure 7), the blowing-mixture injection pressure reached 0.67 MPa. At the same time, roof subsidence was recorded on the injection-well side. A pressure of 0.67 MPa was applied for 5.5 h. The average combustible gas concentration was 39%. Measurements of the combustion product composition showed that CO₂ is a significant component of the producer gas.

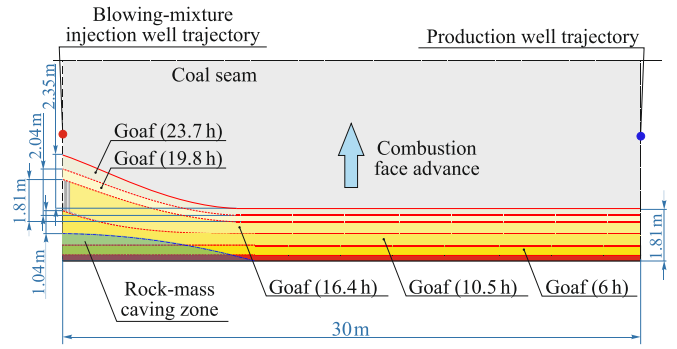


Figure 7. Schematic of combustion face advance at coal seam thickness $m = 1.2$ m, blowing-mixture injection pressure $P = 0.65$ MPa, and gasification duration $t = 23.7$ h

The CO concentration includes the contribution from the primary reaction, where CO is formed in the oxidizing zone. During the secondary reaction, CO is formed in the reducing zone involving carbon dioxide and carbon at gasifier channel wall temperatures of 800-1200°C. The CO content increases along the channel. After that, roof subsidence was recorded at different points of the seam roof, as shown in Figure 8.

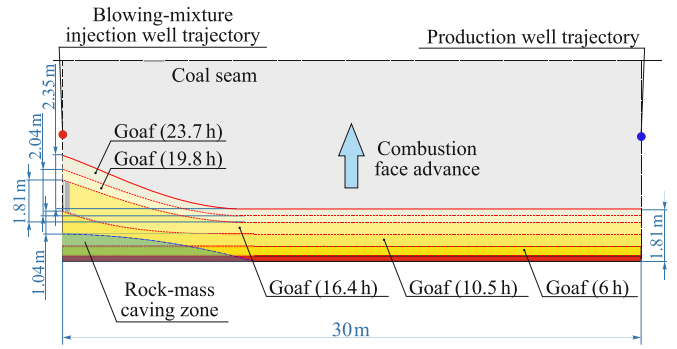


Figure 8. Schematic of combustion face advance at coal seam thickness $m = 1.2$ m; blowing-mixture injection pressure $P = 0.45$ MPa; and gasification duration $t = 29.2$ h

Analysis of the data in Figure 8 indicates a decrease in the gasified space area. This decrease is associated with roof-rock caving that occurs at a specific step along the combustion face. Roof caving is non-uniform. In the reducing zone, the caving step varies from 1.23 to 1.37 m. In the oxidizing zone, it ranges from 1.4 to 2.75 m. The non-uniformity of the caving step is primarily due to temperature effects on the rock mass. During gasification of coal seams with thicknesses from 0.6 to 1.0 m, the caving-step parameters are similar. This indicates that temperature plays a decisive role in the roof-caving mechanisms. The obtained caving-step values are consistent with parameters reported previously [67, 68].

After roof caving was observed during the experiments, it was decided to reduce the blowing-mixture injection pressure to 0.4 MPa. During further gasification, after 11.2 h, the gas concentration decreased to 36.8%. When the pressure was increased to 0.47 MPa, the gas concentration began to rise. The same pattern was observed during gasification of seams with thicknesses from 0.6 to 1.0 m. At each stage of the experiments, four pressure-increase steps were recorded. These adjustments were made in response to changes in the gasified space size during the gasification process. Figure 9 presents the variation of the gasified space area S with gasification duration t and coal seam thickness m .

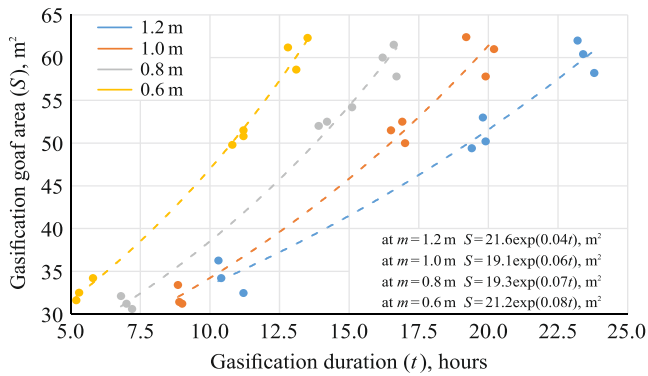


Figure 9. Relationships between the gasified space area and gasification duration and coal seam thickness

Analysis of the data in Figure 9 indicates an exponential increase in the gasified space area with gasification duration.

The established relationships enable the prediction of the gasified space expansion parameters as a function of gasification duration. They can also support controlled adjustment of underground coal gasification operating regimes, which improves process stability and efficiency.

4.3. Synthesis and implications for UCG process control and roof stability

The measured temperature pattern in the immediate roof along the combustion face reflects the canonical spatial separation of reaction zones in underground coal gasification. In UCG, the oxidizing zone near the injection side is dominated by exothermic oxidation reactions, which provide most of the heat input. Further downstream, the reducing zone is governed by endothermic gasification reactions that progressively consume heat, thereby reducing the thermal driving force for conductive heating of the surrounding rock mass. This zonation and the associated nonuniform heat release are widely reported as the main reasons for an asymmetric temperature field around the UCG reactor and for the presence of localized high gradients near the interface between exothermic and endothermic intervals [24, 69-71].

A key point for interpretation is that the temperatures reported in this study were registered in the roof rocks at 0.55 m above the coal seam rather than inside the reaction channel. Therefore, the absolute values in the roof are expected to be substantially lower than the commonly reported peak temperatures inside the UCG cavity, which may reach about 1000-1200°C depending on the operating regime and coal type. The observed maximum in the roof near the transition zone is nevertheless consistent with the general understanding that the highest thermal loading on the surrounding rocks is typically associated with the moving combustion front and the region of most intense change in reaction rate [24, 69, 70, 72].

The strength response of the immediate roof siltstone, namely a pronounced increase in uniaxial compressive strength toward the transition zone, followed by a decrease toward the production side, can be explained by competing temperature-driven mechanisms well known from high-temperature rock mechanics [73]. Many sedimentary rocks exhibit an initial strengthening stage as temperature increases, which is often attributed to dehydration, reduction of free and bound water, and changes in intergranular contacts that can temporarily increase stiffness and peak strength. With further thermal exposure, microcrack initiation and growth

become dominant, driven by thermal expansion mismatch among mineral phases, thermal fatigue, and thermochemical alteration, which ultimately reduce strength and increase deformability. Comprehensive reviews and recent high-temperature datasets for siliciclastic rocks support this non-linearity and the existence of temperature windows where strengthening and weakening may alternate depending on mineralogy, texture, and porosity [74, 75].

In the context of the present results, the peak strength near the transition zone is plausibly associated with the “strengthening-dominated” stage in the roof rock at the investigated offset distance. At the same time, the proximity of the peak temperature to ~573°C is noteworthy because it coincides with the α - β transition of quartz, which is often implicated in microcrack development and subsequent degradation in quartz-bearing rocks [76]. This supports the interpretation that the transition zone is not only the location of maximum thermal loading but also a likely trigger for accelerated damage accumulation. The downstream reduction in UCS toward the reducing zone can then be interpreted as the net effect of accumulated microdamage under repeated or prolonged heating and cooling, combined with stress redistribution caused by the evolving gasification goaf geometry [77, 78].

The dynamics of gasification goaf growth observed in the laboratory, including periods of rapid expansion and episodic decreases in effective area due to roof collapse, are consistent with the established concept that UCG cavity evolution is controlled by both chemical conversion of coal and thermo-mechanical failure of the surrounding materials. Cavity growth mechanisms discussed in the UCG literature typically include coal consumption, spalling from cavity walls and roof, rubble accumulation, and intermittent roof falls, which together produce a strongly nonlinear evolution of cavity shape and hydraulic connectivity. This nonlinearity is a core reason why many authors emphasize coupled thermo-mechanical modeling for predicting roof deformation, stress redistribution, and subsidence trends around UCG reactors [70, 71, 78-80].

The observed linkage between adjustments in blowing-mixture injection pressure and combustible gas concentration is also consistent with prior experimental and modelling studies. Laboratory UCG studies have demonstrated that operational changes in oxidant and steam delivery affect local temperatures, reaction rates, and, consequently, the syngas composition, including the balance between CO, H₂, CH₄, and CO₂. In particular, the expected roles of secondary reactions in the reducing zone, such as the Boudouard and water-gas reactions, provide a mechanistic explanation for changes in CO and H₂ yields along the reactor length. This supports the practical conclusion that process controllability requires adaptive operating regimes that respond to evolving goaf geometry and flow paths rather than fixed setpoints [66, 81-83].

From an engineering perspective, the combined trends in temperature and strength identified here highlight a critical implication for UCG design and monitoring. Even when the immediate roof experiences moderate temperatures relative to the cavity interior, localized gradients near the transition zone can produce the most pronounced changes in mechanical behaviour. Because cavity evolution and roof response are coupled, the gasification goaf geometry should be treated as a dynamic state variable in process control and in geomechanical risk assessment, particularly when evaluating the likelihood of roof falls that may alter permeability pathways and affect environmental containment.

- [8] Pavlychenko, A., & Kovalenko, A. (2013). The investigation of rock dumps influence to the levels of heavy metals contamination of soil. *Annual Scientific-Technical Collection – Mining of Mineral Deposits*, 237-238. <https://doi.org/10.1201/b16354-43>
- [9] Gorova, A., Pavlychenko, A., Kulyna, S., & Shkremetko, O. (2012). Ecological problems of post-industrial mining areas. *Geomechanical Processes During Underground Mining*, 35-40. <https://doi.org/10.1201/b13157-7>
- [10] Hu, H. (2025). Research Progress and Future Development Direction of Deep Underground Coal Gasification. *Combustion Science and Technology*, 1-24. <https://doi.org/10.1080/00102202.2025.2534442>
- [11] Cui, C., Liu, Y., Chai, X., & Tian, L. (2025). Investigation on performance characteristics and thermal analysis of underground coal gasification in porous media based on non-steady flow. *Fuel*, 389, 134629. <https://doi.org/10.1016/j.fuel.2025.134629>
- [12] Li, H., Cao, J., Tang, C., Guo, G., Chen, Y., Zha, J., Huang, W., Yuan, Y., & Huang, J. (2025). Methods for enhancing resource recovery efficiency in underground coal gasification to promote its large-scale utilization. *Geomechanics for Energy and the Environment*, 41, 100651. <https://doi.org/10.1016/j.gete.2025.100651>
- [13] Falshtynskiy, V.S., Dychkovskiy, R.O., Lozynskiy, V.H., Saik, P.B., & Lozynska, M.I. (2025). Substantiating applicability of Western Donbas coal seams (Ukraine) for underground coal gasification. *Engineering Journal of Satbayev University*, 147(1), 31-42. <https://doi.org/10.51301/vest.su.2025.i1.05>
- [14] Bondarenko, V., Lozynskiy, V., Sai, K., & Anikushyna, K. (2015). An overview and prospectives of practical application of the biomass gasification technology in Ukraine. *New Developments in Mining Engineering 2015: Theoretical and Practical Solutions of Mineral Resources Mining*, 27-32. <https://doi.org/10.1201/b19901-6>
- [15] Salieiev, I., Bondarenko, V., Kovalevska, I., Malashkevych, D., & Galkov, R. (2025). Principles of mining-geological classification for maintaining mine workings in conditions of weakly metamorphosed rocks. *Mining of Mineral Deposits*, 19(1), 26-36. <https://doi.org/10.33271/mining19.01.026>
- [16] Lozynskiy, V. (2025). Multi-criteria assessment of coal seams suitability for co-gasification using the preference selection index. *Heliyon*, 11(10), e43368. <https://doi.org/10.1016/j.heliyon.2025.e43368>
- [17] Dychkovskiy, R., Dyczko, A., & Borojević Šostarić, S. (2024). Foreword: Physical and Chemical Geotechnologies – Innovations in Mining and Energy. *E3S Web of Conferences*, 567, 00001. <https://doi.org/10.1051/e3sconf/202456700001>
- [18] Sakhno, I., Sakhno, S., & Vovna, O. (2025). Surface Subsidence Response to Safety Pillar Width Between Reactor Cavities in the Underground Gasification of Thin Coal Seams. *Sustainability*, 17(6), 2533. <https://doi.org/10.3390/su17062533>
- [19] Fedoreiko, V., Kravchenko, O., Sala, D., Zahorodnii, R., Pyzalski, M., & Dychkovskiy, R. (2026). Management and Optimization of Bio-Resource Decentralized Energy Generation Under Political Instability. *Energies*, 19(3), 737. <https://doi.org/10.3390/en19030737>
- [20] Lysyi, N., Helesh, A., Popovych, V., Saik, P., & Dmytruk, O. (2025). Thermodynamic research of coal mining waste gasification processes. *Mining of Mineral Deposits*, 19(3), 132-143. <https://doi.org/10.33271/mining19.03.132>
- [21] Lozynskiy, V., Saik, P., Petlovanyi, M., Sai, K., Malanchuk, Z., & Malanchuk, Y. (2018). Substantiation into mass and heat balance for underground coal gasification in faulting zones. *Inzynieria Mineralna*, 19(2), 289-300. <https://doi.org/10.29227/IM-2018-02-36>
- [22] Perkins, G. (2018). Underground coal gasification – Part I: Field demonstrations and process performance. *Progress in Energy and Combustion Science*, 67, 158-187. <https://doi.org/10.1016/j.peccs.2018.02.004>
- [23] Saik, P., Lozynskiy, V., Anisimov, O., Akimov, O., Kozhantov, A., & Mamaykin, O. (2023). Managing the process of underground coal gasification. *Naukovyi Visnyk Natsionalnoho Hirnychoho Universytetu*, (6), 25-30. <https://doi.org/10.33271/nvngu/2023-6/025>
- [24] Bhattu, A.W., Bazmi, A.A., & Zahedi, G. (2013). Underground coal gasification: From fundamentals to applications. *Progress in Energy and Combustion Science*, 39(1), 189-214. <https://doi.org/10.1016/j.peccs.2012.09.004>
- [25] Tomás, R., Benavente, D., Martínez-Ibáñez, V., & Garrido, M. E. (2025). How do high temperatures affect rock properties? A comprehensive review of experimental thermal effects and underlying mechanisms. *Engineering Geology*, 357, 108323. <https://doi.org/10.1016/j.enggeo.2025.108323>
- [26] Ding, Q.L., Wang, P., & Cheng, Z. (2021). Influence of temperature and confining pressure on the mechanical properties of granite. *Powder Technology*, 394, 10-19. <https://doi.org/10.1016/j.powtec.2021.08.036>
- [27] Jin, J., Liu, J., Chen, W., Li, G., Cheng, W., Zhang, X., & Luo, Y. (2024). The impact of high temperature on mechanical properties and behaviors of sandstone. *Frontiers in Earth Science*, 12, 1322495. <https://doi.org/10.3389/feart.2024.1322495>
- [28] Bondarenko, V.I., Salieiev, I.A., Kovalevska, I.A., Vivcharenko, I.O., & Sheka, I.V. (2025). Substantiation of geomechanical principles for predicting outgassing during complex mining of mineral raw materials. *Mineral Resources of Ukraine*, (3), 10-16. <https://doi.org/10.31996/mru.2025.3.10-16>
- [29] Abdiev, A.R., Wang, J., Mambetova, R.S., Abdiev, A.A., & Abdiev, A.S. (2025). Geomechanical assessment of stress-strain conditions in structurally heterogeneous rock masses of Kyrgyzstan. *Engineering Journal of Satbayev University*, 147(2), 31-39. <https://doi.org/10.51301/ejsu.2025.i2.05>
- [30] Kačur, J., & Kostúr, K. (2017). Approaches to the gas control in UCG. *Acta Polytechnica*, 57(3), 182-200. <https://doi.org/10.14311/ap.2017.57.0182>
- [31] Lozynskiy, V. (2024). Numerical simulation of carbonaceous raw material combustion in a coal seam channel. *Mining of Mineral Deposits*, 18(4), 109-124. <https://doi.org/10.33271/mining18.04.109>
- [32] Xiao, Y., Yin, J., Hu, Y., Wang, J., Yin, H., & Qi, H. (2019). Monitoring and Control in Underground Coal Gasification: Current Research Status and Future Perspective. *Sustainability*, 11(1), 217. <https://doi.org/10.3390/su11010217>
- [33] Saik, P.B., Dychkovskiy, R.O., Lozynskiy, V.G., Malanchuk, Z.R., & Malanchuk, Ye.Z. (2016). Revisiting the underground gasification of coal reserves from contiguous seams. *Naukovyi Visnyk Natsionalnoho Hirnychoho Universytetu*, (6), 60-66.
- [34] Pershad, S., Pistorius, J., & van der Riet, M. (2018). Majuba underground coal gasification project. *Underground Coal Gasification and Combustion*, 469-502. <https://doi.org/10.1016/b978-0-08-100313-8.00014-1>
- [35] Saik, P.B., & Berdnyk, M.H. (2024). Mathematical model for heat transfer during underground coal gasification process. *Naukovyi Visnyk Natsionalnoho Hirnychoho Universytetu*, (5), 19-24. <https://doi.org/10.33271/nvngu/2024-5/019>
- [36] Lozynskiy, V. (2023). Critical review of methods for intensifying the gas generation process in the reaction channel during underground coal gasification (UCG). *Mining of Mineral Deposits*, 17(3), 67-85. <https://doi.org/10.33271/mining17.03.067>
- [37] Svetkina, Y., Falshtyn'skyy, V., & Dychkov'skyy, R. (2010). Features of selectivity process of borehole underground coal gasification. *New Techniques and Technologies in Mining*, 219-222.
- [38] Saik, P., & Berdnyk, M. (2024). mathematical model of temperature distribution in rock sample during heating. *Scientific papers of DonNTU Series: "The Mining and Geology."* 1(31)-2(32), 70-77. [https://doi.org/10.31474/2073-9575-2024-1\(31\)-2\(32\)-70-77](https://doi.org/10.31474/2073-9575-2024-1(31)-2(32)-70-77)
- [39] Fang, H., Liu, Y., Ge, T., Zheng, T., Yu, Y., Liu, D., Ding, J., & Li, L. (2022). A Review of Research on Cavity Growth in the Context of Underground Coal Gasification. *Energies*, 15(23), 9252. <https://doi.org/10.3390/en15239252>
- [40] Khan, M., Mmbaga, J., Shirazi, A., Trivedi, J., Liu, Q., & Gupta, R. (2015). Modelling Underground Coal Gasification – A Re-

- view. *Energies*, 8(11), 12603-12668. <https://doi.org/10.3390/en81112331>
- [41] Falshtynskiy, V., Lozynskiy, V., Saik, P., Dychkovskiy, R., & Tabachenko, M. (2016). Substantiating parameters of stratification cavities formation in the roof rocks during underground coal gasification. *Mining of Mineral Deposits*, 10(1), 16-24. <https://doi.org/10.15407/mining10.01.016>
- [42] Saik, P., & Yankin, D. (2025). On the issue of the rational planning of mining operations for underground coal gasification. *Collection of Research Papers of the National Mining University*, 80, 81-92. <https://doi.org/10.33271/crpnmu/80.081>
- [43] Laciak, M., Kačur, J., & Durdán, M. (2022). Modeling and Control of Energy Conversion during Underground Coal Gasification Process. *Energies*, 15(7), 2494. <https://doi.org/10.3390/en15072494>
- [44] Dreus, A.Yu., Sudakov, A.K., Kozhevnikov, A.A., & Vakhalin, Yu.N. (2016). Study on thermal strength reduction of rock formation in the diamond core drilling process using pulse flushing mode. *Naukovyi Visnyk Natsionalnoho Hirnychoho Universytetu*, (3), 5-10.
- [45] Lu, Y., & Cha, M. (2022). Thermally induced fracturing in hot dry rock environments-Laboratory studies. *Geothermics*, 106, 102569. <https://doi.org/10.1016/j.geothermics.2022.102569>
- [46] Shahbazi, M., Najafi, M., Fatehi Marji, M., & Abdollahipour, A. (2025). Thermo-Mechanical Analysis of Crack Propagation Process in Heterogeneous Brittle Coal and Its Effects on the UCG Cavity Growth Rate. *Energy Science & Engineering*, 13(3), 1062-1078. <https://doi.org/10.1002/ese3.2002>
- [47] Xin, L., Li, H., Niu, M., Yang, M., Xu, W., Wang, X., & Diao, T. (2025). Experimental and numerical investigation of thermal cracking of overlying rock in underground coal gasification. *Engineering Fracture Mechanics*, 315, 110808. <https://doi.org/10.1016/j.engfracmech.2025.110808>
- [48] Wu, J., Xu, H., Cao, C., Chen, Y., Xin, F., & Yin, Z. (2026). A novel method for predicting permeability in quartz-bearing rocks at high temperatures during underground coal gasification. *Fuel*, 404, 136195. <https://doi.org/10.1016/j.fuel.2025.136195>
- [49] Bukowska, M., & Sygala, A. (2015). Deformation properties of sedimentary rocks in the process of underground coal gasification. *Journal of Sustainable Mining*, 14(3), 144-156. <https://doi.org/10.1016/j.jsm.2015.11.003>
- [50] Chepiga, D., Podkopaiev, S., Gogo, V., Shashenko, O., Skobenko, O., Demchenko, O., & Podkopayev, Y. (2024). Dualistic effect of the deformation of protective structures made of broken rock in mine workings under static load. *Mining of Mineral Deposits*, 18(2), 122-131. <https://doi.org/10.33271/mining18.02.122>
- [51] Liu, S., Zhang, S., Chen, F., Wang, C., & Liu, M. (2014). Variation of coal permeability under dehydrating and heating: a case study of ulanqab lignite for underground coal gasification. *Energy & Fuels*, 28(11), 6869-6876. <https://doi.org/10.1021/ef501696e>
- [52] Ma, H., Song, Y., Yang, J., Zheng, J., Shen, F., & Shao, Z. (2023). Experimental investigation on acoustic emission and damage characteristics of dehydrated lignite in uniaxial compression test. *Bulletin of Engineering Geology and the Environment*, 82(8), 292. <https://doi.org/10.1007/s10064-023-03315-z>
- [53] Luo, J., & He, J. (2022). Mechanical characteristics of sandstone under high temperature and cyclic loading in underground coal gasification. *Minerals*, 12(10), 1313. <https://doi.org/10.3390/min12101313>
- [54] Feng, G., Wang, X., Kang, Y., Luo, S., & Hu, Y. (2019). Effects of temperature on the relationship between mode-I fracture toughness and tensile strength of rock. *Applied Sciences*, 9(7), 1326. <https://doi.org/10.3390/app9071326>
- [55] Zhang, L., Mao, X., & Lu, A. (2009). Experimental study on the mechanical properties of rocks at high temperature. *Science in China Series E: Technological Sciences*, 52(3), 641-646. <https://doi.org/10.1007/s11431-009-0063-y>
- [56] Yavuz, H., Demirdag, S., & Caran, S. (2010). Thermal effect on the physical properties of carbonate rocks. *International Journal of Rock Mechanics and Mining Sciences*, 47(1), 94-103. <https://doi.org/10.1016/j.ijrmms.2009.09.014>
- [57] Sygala, A., Bukowska, M., & Janoszek, T. (2021). High temperature versus geomechanical parameters of selected rocks – the present state of research. *Journal of Sustainable Mining*, 12(4), 9. <https://doi.org/10.46873/2300-3960.1291>
- [58] Chen, Y.-L., Ni, J., Shao, W., & Azzam, R. (2012). Experimental study on the influence of temperature on the mechanical properties of granite under uniaxial compression and fatigue loading. *International Journal of Rock Mechanics and Mining Sciences*, 56, 62-66. <https://doi.org/10.1016/j.ijrmms.2012.07.026>
- [59] Korzeniowski, W., & Skrzypkowski, K. (2012). Investigations of changes of selected geo-mechanical properties of rocks under the influence of temperature up to 1100 °C in the aspect of potential underground coal gasification process. *Przegląd Gorniczy*, (68), 44-53.
- [60] Zhang, L., Mao, X., Liu, R., Guo, X., & Ma, D. (2013). The mechanical properties of mudstone at high temperatures: an experimental study. *Rock Mechanics and Rock Engineering*, 47(4), 1479-1484. <https://doi.org/10.1007/s00603-013-0435-2>
- [61] Małkowski, P., Niedbalski, Z., & Hydzik-Wiśniewska, J. (2013). Zmiany właściwości strukturalnych i cieplnych skał poddanych wysokim temperaturom w rejonie projektowanego georeaktora. *Archives of Mining Sciences*, 58(2), 465-480. <https://doi.org/10.2478/amsc-2013-0031>
- [62] Mao, X., Zhang, L., Li, T., & Liu, H. (2009). Properties of failure mode and thermal damage for limestone at high temperature. *Mining Science and Technology (China)*, 19(3), 290-294. [https://doi.org/10.1016/s1674-5264\(09\)60054-5](https://doi.org/10.1016/s1674-5264(09)60054-5)
- [63] Guo, J., Lei, Y., Yang, Y., Cheng, P., Wang, Z., & Wu, S. (2023). Effects of high temperature treatments on strength and failure behavior of sandstone under dynamic impact loads. *Sustainability*, 15(1), 794. <https://doi.org/10.3390/su15010794>
- [64] Bukowska, M., & Sygala, A. (2021). Deformation properties of sedimentary rocks in the process of underground coal gasification. *Journal of Sustainable Mining*, 14(3). <https://doi.org/10.46873/2300-3960.1239>
- [65] Brovko, D., Makareiko, R., Sakhno, S., Yanova, L., & Pischikova, O. (2024). Modeling the stability of air flows in inclined workings in case of fire. *Mining of Mineral Deposits*, 18(3), 52-62. <https://doi.org/10.33271/mining18.03.052>
- [66] Dychkovskiy, R., Falshtynskiy, V., Saik, P., Lozynskiy, V., Sala, D., Hankus, Ł., Magdziarczyk, M., & Smoliński, A. (2025). Control of contour evolution, burn rate variation, and reaction channel formation in coal gasification. *Scientific Reports*, 15(1). <https://doi.org/10.1038/s41598-025-93611-3>
- [67] Kadirov, V.R., Nurboboiev, Y.T., Umirzoqov, A.A., Muhammadiyev Elbek (2022). Rock displacement at underground coal gasification. *International Journal on Human Computing Studies*, 1(4), 72-82. <https://doi.org/10.31149/ijhcs.v4i1.2688>
- [68] Bondarenko, V., Dychkovskiy, R., & Falshtynskiy, V. (2009). Synthetic stowing of rockmass at borehole underground coal gasification (BUGG). *Deep Mining Challenges*, 169-177. <https://doi.org/10.1201/NOE0415804288-24>
- [69] Couch, G.R. (2009). Underground coal gasification. IEA Clean Coal Centre, London, UK. Report No. *Contract No.: CCC/151*, 129.
- [70] Perkins, G. (2018). Underground coal gasification—Part II: Fundamental phenomena and modeling. *Progress in Energy and Combustion Science*, 67, 234-274. <https://doi.org/10.1016/j.peccs.2018.03.002>
- [71] Yang, D., Sarhosis, V., & Sheng, Y. (2014). Thermal-mechanical modelling around the cavities of underground coal gasification. *Journal of the Energy Institute*, 87(4), 321-329. <https://doi.org/10.1016/j.joei.2014.03.029>
- [72] Prabu, V., & Jayanti, S. (2014). Heat-affected zone analysis of high ash coals during ex situ experimental simulation of underground coal gasification. *Fuel*, 123, 167-174. <https://doi.org/10.1016/j.fuel.2014.01.035>

- [73] Ishchenko, O., Novikov, L., Ponomarenko, Y., Konoval, V., Kinasz, R., & Ishchenko, K. (2026). Research into fracture mechanism of complex-structured crystalline mass under triaxial compression. *Mining of Mineral Deposits*, 20(1), 1-12. <https://doi.org/10.33271/mining20.01.001>
- [74] Zhang, Y., Zhang, C., Jia, J., & Zhou, C. (2024). Experimental investigation of high-temperature effects on the physical and mechanical properties of granite, sandstone, and limestone. *Applied Energy*, 357, 122532. <https://doi.org/10.1016/j.apenergy.2023.122532>
- [75] Birawidha, D.C., Amin, M., Miswanto, A., Jaya, F.H., Dewi, S.U., Nariswari, M.K., & Putri, D.M. (2025). Variations in alumina-based material composition and heating temperature of refractory bricks in mullite formation. *Mining of Mineral Deposits*, 19(4), 130-138. <https://doi.org/10.33271/mining19.04.130>
- [76] Peng, Z., & Redfern, S.A.T. (2013). Mechanical properties of quartz at the α - β phase transition: Implications for tectonic and seismic anomalies. *Geochemistry, Geophysics, Geosystems*, 14(1). doi: <https://doi.org/10.1029/2012GC004482>
- [77] Elahi, S. M., Nassir, M., & Chen, Z. (2017). Effect of various coal constitutive models on coupled thermo-mechanical modeling of underground coal gasification. *Journal of Petroleum Science and Engineering*, 154, 469-478. <https://doi.org/10.1016/j.petrol.2017.02.016>
- [78] Otto, C., & Kempka, T. (2015). Thermo-Mechanical Simulations of Rock Behavior in Underground Coal Gasification Show Negligible Impact of Temperature-Dependent Parameters on Permeability Changes. *Energies*, 8(6), 5800-5827. <https://doi.org/10.3390/en8065800>
- [79] Daggupati, S., Mandapati, R. N., Mahajani, S. M., Ganesh, A., Mathur, D. K., Sharma, R. K., & Aghalayam, P. (2010). Laboratory studies on combustion cavity growth in lignite coal blocks in the context of underground coal gasification. *Energy*, 35(6), 2374-2386. <https://doi.org/10.1016/j.energy.2010.02.015>
- [80] Prabu, V., & Jayanti, S. (2014). Heat-affected zone analysis of high ash coals during ex situ experimental simulation of underground coal gasification. *Fuel*, 123, 167-174. <https://doi.org/10.1016/j.fuel.2014.01.035>
- [81] Falshtynskyi, V., & Dychkovskyi, R. (2014). Some aspects of technological processes control of an in-situ gasifier during coal seam gasification. *Progressive Technologies of Coal, Coalbed Methane, and Ores Mining*, 109-112. <https://doi.org/10.1201/b17547-20>
- [82] Daggupati, S., Mandapati, R.N., Mahajani, S.M., Ganesh, A., Sapru, R.K., Sharma, R.K., & Aghalayam, P. (2011). Laboratory studies on cavity growth and product gas composition in the context of underground coal gasification. *Energy*, 36(3), 1776-1784. <https://doi.org/10.1016/j.energy.2010.12.051>
- [83] Kumari, G., & Vairakannu, P. (2017). Laboratory scale studies on CO₂ oxy-fuel combustion in the context of underground coal gasification. *Journal of CO₂ Utilization*, 21, 177-190. <https://doi.org/10.1016/j.jcou.2017.06.021>

Температуралық-беріктік өзгерістердің тікелей төбе жыныстарындағы динамикасы және жерасты газ генераторы астындағы газсызданған кеңістіктің қалыптасуы

П. Саик^{1,2}, В. Лозинский^{1,2*}, М. Берник¹, Д. Климов¹

¹«Бір бел, бір жол» бастамасы Қытай-Еуропа зерттеулер орталығы (BRICCES), Гуандунь мұнай-химия технологиялары университеті, Маомин, Қытай

²Ұлттық «Днепровск политехникасы» техникалық университеті, Днепр, Украина

*Корреспонденция үшін автор: lozynskiy.v.h@nmu.one

Андатпа. Жұмыстың мақсаты – отты кенжарбойындағы химиялық реакциялар аймақтарының әсерінен тікелей төбе жыныстарының температуралық өрісі мен беріктігінің өзгеру заңдылықтарын анықтау, сондай-ақ газификацияның ұзақтығына, үрлеу қоспасын беру қысымына және көмір қабатының қалыңдығына байланысты газсызданған кеңістік ауданының уақыт бойынша қалыптасуы мен өзгеру тәуелділіктерін белгілеу. Зерттеулер отты кенжар фронтының ілгерілеуі мен төбе жыныстары деформацияларын қайта жаңғырта отырып, жерасты газификациясының зертханалық қондырғысында орындалды. Модельденген тікелей төбеде температура реакциялық арна бойымен термодатчиктер арқылы тіркелді. Украина, «Львовуголь» МК (ГП) құрамындағы «Межиричанская» шахтасының n_7^H қабатының тікелей төбесінен алынған алевролит үлгілері термиялық өңдеуден өткізіліп, KL 200/CE-Tecnotest прессінде бірсытты сығуға сынақтан өткізілді. Газсызданған кеңістіктің геометриясы төбенің төмен түсуін өлшейтін реперлік датчиктер деректері, әртүрлі уақыт мезеттеріндегі контурларды графикалық визуализациялау және генераторлық газдың құрамы мен концентрациясын ескере отырып, трапециялар әдісімен ауданды есептеу негізінде анықталды. n_7^H қабатынан 0,55 м қашықтықта тотығу аймағында (0–9 м) температура шамамен 323-тен 550°C-қа дейін өсетіні, өтпелі аймақта (9–11 м) шамамен 573°C-қа жететіні, ал қалпына келтіру аймағында (11–30 м) ~200°C-қа дейін төмендейтіні анықталды. Алевролиттердің беріктігі кенжар бойымен өтпелі аймақ маңында максимумға жетіп, кейін қалпына келтіру аймағында азаяды; бұл ретте тотығу аймағы үшін экспоненциалдық, ал қалпына келтіру аймағы үшін логарифмдік тәуелділік тән. Газсызданған кеңістік ауданының газификация ұзақтығына және қабат қалыңдығына байланысты сызықтық емес, негізінен экспоненциалды түрде өзгеретіні және үрлеу қоспасын беру қысымы режимімен әрі төбе жыныстарының құлау көріністерімен байланысты екені көрсетілді. Алынған заңдылықтар жерасты газификациясының басқарылатын режимдерін негіздеу кезінде газсызданған кеңістік параметрлерін болжау және төбенің орнықтылығын бағалау үшін пайдаланылуы мүмкін.

Негізгі сөздер: көмірдің жерасты газификациясы, газсызданған кеңістік, температуралық өріс, тау жыныстары, бірсытты сығуға беріктік, отты кенжар.

Динамика температурно-прочностных изменений непосредственной кровли и формирование выгазованного пространства подземного газогенератора

П. Саик^{1,2}, В. Лозинский^{1,2*}, М. Берник¹, Д. Климов¹

¹Центр китайско-европейских исследований инициативы «Пояс и путь» (BRICCES), Гуандунский университет нефтехимических технологий, Маолин, Китай

²Национальный технический университет «Днепропетровская политехника», Днепр, Украина

*Автор для корреспонденции: lozynskiy.v.h@nmu.one

Аннотация. Целью работы является установление закономерностей изменения температурного поля и прочности пород непосредственной кровли под воздействием зон химических реакций вдоль огневого забоя, а также определение зависимостей формирования и изменения площади выгазованного пространства во времени в зависимости от продолжительности газификации, давления подачи дутьевой смеси и мощности угольного пласта. Исследования выполнены на лабораторной установке подземной газификации с воспроизведением продвижения фронта огневого забоя и деформаций кровли. Температуру в смоделированной непосредственной кровле регистрировали термодатчиками вдоль реакционного канала. Образцы алевролитов из непосредственной кровли пласта n_7^H шахты «Межиричанская» (ГП «Львовуголь», Украина) подвергали термообработке и испытывали на одноосное сжатие на прессе KL 200/CE-Tecnotest. Геометрию выгазованного пространства определяли по данным реперных датчиков опускания кровли, графической визуализации контуров в различные моменты времени и расчета площади методом трапеций с учетом состава и концентрации генераторного газа. Установлено, что на расстоянии 0,55 м от пласта температура в окислительной зоне (0-9 м) возрастает примерно от 323 до 550°C, в переходной зоне (9-11 м) достигает около 573°C, а в восстановительной зоне (11-30 м) снижается до ~200°C. Прочность алевролитов изменяется вдоль забоя с максимумом в районе переходной зоны и последующим уменьшением в восстановительной зоне, причем для окислительной зоны характерна экспоненциальная, а для восстановительной – логарифмическая зависимость. Показано, что площадь выгазованного пространства изменяется нелинейно, преимущественно экспоненциально, в зависимости от продолжительности газификации и мощности пласта и связана с режимом давления подачи дутьевой смеси и проявлениями обрушения пород кровли. Полученные закономерности могут быть использованы для прогнозирования параметров выгазованного пространства и оценки устойчивости кровли при обосновании управляемых режимов подземной газификации.

Ключевые слова: подземная газификация угля; выгазованное пространство; температурное поле; горные породы; прочность на одноосное сжатие; огневой забой.

Publisher's note

All claims expressed in this manuscript are solely those of the authors and do not necessarily represent those of their affiliated organizations, or those of the publisher, the editors and the reviewers.